

Experimental Section

A vial equipped with a septum screw-cap and a stir bar was purged with argon. The olefin (1.20 mmol, 1.20 equiv) and then a solution of 9-BBN (0.50 M in THF; 2.40 mL, 1.20 mmol, 1.20 equiv) were introduced to the vial, and the resulting homogeneous solution was stirred for at least 6 hours at room temperature. After that time, the THF was removed under vacuum and replaced with dioxane (0.9 mL).^[16] In air, a stir bar, $[\text{Pd}_2(\text{dba})_3]$ (45.8 mg, 0.05 mmol, 5%), PCy_3 (56.0 mg, 0.20 mmol, 20%), and $\text{CsOH} \cdot \text{H}_2\text{O}$ (185 mg, 1.10 mmol, 1.10 equiv) were placed into a second vial, which was then capped with a septum screw-cap and purged with argon for 10 minutes. Dioxane (0.3 mL) was added by syringe, and then the solution of the alkyl-9-BBN was added through a cannula (the alkyl-9-BBN was transferred completely by rinsing the first vial with dioxane (2×0.3 mL)). The alkyl chloride (1.00 mmol, 1.00 equiv) was introduced to this homogeneous brown solution, and the resulting mixture was stirred vigorously under argon for 48 hours at 90 °C. At the conclusion of the coupling, the reaction mixture, which was now heterogeneous, was cooled to room temperature, diluted with Et_2O (5 mL), and filtered through a short plug of silica gel with Et_2O washings (30 mL). The solvent was evaporated, and the resulting yellow residue was purified by flash chromatography.

Received: March 15, 2002 [Z18905]

- [1] *Metal-Catalyzed Cross-Coupling Reactions* (Eds.: F. Diederich, P. J. Stang), Wiley-VCH, New York, **1998**.
- [2] For reviews, see: a) T.-Y. Luh, M.-K. Leung, K.-T. Wong, *Chem. Rev.* **2000**, *100*, 3187–3204; b) D. J. Cárdenas, *Angew. Chem.* **1999**, *111*, 3201–3203; *Angew. Chem. Int. Ed.* **1999**, *38*, 3018–3020.
- [3] T. Ishiyama, S. Abe, N. Miyauchi, A. Suzuki, *Chem. Lett.* **1992**, 691–694.
- [4] For reviews of the Suzuki reaction, see: a) A. Suzuki in *Metal-Catalyzed Cross-Coupling Reactions* (Eds.: F. Diederich, P. J. Stang), Wiley-VCH, New York, **1998**; chap. 2; b) N. Miyauchi, A. Suzuki, *Chem. Rev.* **1995**, *95*, 2457–2483; c) S. R. Chemler, D. Trauner, S. J. Danishefsky, *Angew. Chem.* **2001**, *113*, 4676–4701; *Angew. Chem. Int. Ed.* **2001**, *40*, 4544–4568.
- [5] Suzuki coupling of alkyl bromides: M. R. Netherton, C. Dai, K. Neuschütz, G. C. Fu, *J. Am. Chem. Soc.* **2001**, *123*, 10099–10100.
- [6] a) A. Devasagayaram, T. Stüdemann, P. Knochel, *Angew. Chem.* **1995**, *107*, 2592–2594; *Angew. Chem. Int. Ed. Engl.* **1995**, *34*, 2723–2725; b) R. Giovannini, T. Stüdemann, G. Dussin, P. Knochel, *Angew. Chem.* **1998**, *110*, 2512–2515; *Angew. Chem. Int. Ed.* **1998**, *37*, 2387–2390; c) R. Giovannini, T. Stüdemann, A. Devasagayaram, G. Dussin, P. Knochel, *J. Org. Chem.* **1999**, *64*, 3544–3553; d) M. Piber, A. E. Jensen, M. Rottländer, P. Knochel, *Org. Lett.* **1999**, *1*, 1323–1326; e) A. E. Jensen, P. Knochel, *J. Org. Chem.* **2002**, *67*, 79–85.
- [7] After our paper was submitted for publication, Kambe et al. reported one example of a nickel-catalyzed Kumada coupling of a simple alkyl chloride: J. Terao, H. Watanabe, A. Ikumi, H. Kuniyasu, N. Kambe, *J. Am. Chem. Soc.* **2002**, *124*, 4222–4223.
- [8] For example, see: J. March, *Advanced Organic Chemistry*, Wiley, New York, **1992**, p. 357.
- [9] J. March, *Advanced Organic Chemistry*, Wiley, New York, **1992**, p. 24.
- [10] If no phosphine is present, no coupling product is detected (<2%).
- [11] With a 1:1 phosphine:palladium ratio, the yield according to GC is ca. 70%; with a 1:2 phosphine:palladium ratio, ca. 60%.
- [12] Each change in parameter leads to a change in yield of ≈ 15 –25%.
- [13] Lower yields are observed for reactions of more hindered substrates. To date, we have not been able to perform couplings of secondary alkyl chlorides or secondary alkyl boranes.
- [14] When 1.0 equiv of $\text{CsOH} \cdot \text{H}_2\text{O}$ or KOH is added to *n*-octyl-9-BBN ($\delta(^{11}\text{B}) = 89$ ppm) in dioxane at 90 °C, ^{11}B NMR analysis indicates that a soluble $[\text{n-octyl-9-BBN}(\text{OH})]^-$ “ate” complex is quickly formed ($\delta = -1$ for $\text{CsOH} \cdot \text{H}_2\text{O}$; $\delta = 18$ ppm for KOH (equilibrium between three- and four-coordinate boron; the four-coordinate adduct reso-

nates at $\delta = -2$ ppm)). Presumably, this is the species that transfers the *n*-octyl group to palladium (Scheme 1). For ^{11}B NMR investigations of related systems, see: K. Matos, J. A. Soderquist, *J. Org. Chem.* **1998**, *63*, 461–470. See also: R. Köster, G. Seidel, B. Wrackmeyer, *Chem. Ber.* **1992**, *125*, 617–625.

- [15] Use of a less hindered (methyl) ester leads to a lower yield (≈ 55 %).
- [16] If desired, the synthesis of the alkyl-9-BBN can be conducted directly in dioxane by hydroborating the olefin with solid 9-BBN dimer, rather than a solution of 9-BBN in THF (both are commercially available).

Hydrogen Bonding Modulates the Selectivity of Enzymatic Oxidation by P450: Chameleon Oxidant Behavior by Compound I**

Samuël P. de Visser, François Ogliaro, Pankaz K. Sharma, and Sason Shaik*

Two of the important reactions of the enzyme cytochrome P450 are C–H hydroxylation and C=C epoxidation.^[1–5] Different P450 isozymes give different ratios of these products with substrates which can undergo both hydroxylation and epoxidation.^[1] Furthermore, mutation of a single amino acid away from the reaction center changes the ratio of the two products.^[6] What are the factors that determine the oxidation regioselectivity? There may exist many answers^[1–5] to this question and it is desirable to begin unraveling them step by step. Here we use model calculations of C–H hydroxylation and C=C epoxidation pathways, which show that the primary active species of the enzyme, compound I (Cpd I), behaves like a chameleon oxidant that changes its reactivity and selectivity patterns under the influence of hydrogen bonding and polarization effects, which mimic the protein environment.

To explore this issue, we used density functional calculations (see Methods Section) of a model Cpd I species that reacts with propene to give both allylic hydroxylation and C=C epoxidation. The reaction profiles were computed under different conditions, including effects of the environment such as polarization effect and $\text{NH} \cdots \text{S}$ hydrogen bonding of the type found in the crystal structures of P450 enzymes.^[6, 7] Our model calculations, which focus on the electronic component of the environment, do not involve stereoelectronic effects

[*] Prof. S. Shaik, Dr. S. P. de Visser, Dr. F. Ogliaro, Dr. P. K. Sharma
Department of Organic Chemistry and
The Lise Meitner-Minerva Center
for Computational Quantum Chemistry
Hebrew University
91904 Jerusalem (Israel)
Fax: (+972) 2-658-4680
E-mail: sason@yfaat.ch.huji.ac.il

[**] The research was supported in parts by the Israel Science Foundation (ISF), the German Israeli Binational Foundation (GIF), and by the Ministry of Science, Culture, and Sports. F.O. thanks the European community for a Marie Curie Fellowship.

Supporting information for this article is available on the WWW under <http://www.angewandte.com> or from the author.

arising from variations in the substrate,^[1–5, 8] or effects arising from substrate binding and juxtaposition in the enzyme's pocket.^[9, 10]

Figure 1 shows the lowest energy profiles of the two possible reaction pathways for the bare molecules, Cpd I (²**1** and ⁴**1**) and propene. The compounds exhibit two-state-reactivity (TSR), involving quartet high-spin (HS) and doublet low-spin (LS) processes,^[11–13] which have the appearance of stepwise mechanisms. However, while the HS mechanism is truly stepwise with carbon-radical intermediates (⁴**2** and ⁴**4**), possessing barriers for the subsequent C–O bond formation steps, the LS radical species (²**2** and ²**4**) behave as shoulders on the potential energy surface, without significant barriers for the C–O bond formation.^[11, 12]

A major difference between the epoxidation and hydroxylation processes is that the barriers to bond activation, via ⁴**TS1** and ²**TS1** as well as ⁴**TS3** and ²**TS3**, favor epoxidation by 3.1–3.8 kcal mol^{–1}. However, as can be seen from Figure 2 a, upon inclusion of zero point energies (ZPE), the four transition states, ⁴**TS1** and ²**TS1** as well as ⁴**TS3** and ²**TS3**, become almost isoenergetic. The ZPE effect is primarily due to the loss of a high-frequency C–H mode (>3000 cm^{–1}) that becomes imaginary in the hydroxylation transition states, ⁴**TS3** and ²**TS3**, and consequently lowers their ZPE compared with those of the epoxidation transition states. Thus, taking into account only the intrinsic reactivities of the bare molecules, it is expected that Cpd I will have a small preference for C=C epoxidation over C–H hydroxylation, and will generate stereoselective epoxidation products but less stereoselective hydroxylation products (due to the differences in the barriers to C–O bond making via ⁴**TS2** and ⁴**TS4**).

Figure 2 shows the effects of the environment on the relative energies of the transition states for bond activation, ²**TS1** and ⁴**TS1** as well as ²**TS3** and ⁴**TS3**. The environmental effects were chosen^[14] to mimic, albeit naively, the interactions of the thiolate ligand (the cysteinate residue) with the protein pocket.^[7] Accordingly, Figure 2b shows the energies of the transition states when the thiolate ligand is coordinated by two NH···S hydrogen bonds, while Figure 2c shows the effect of a relatively nonpolar, yet polarizing, environment represented by the dielectric constant $\epsilon = 5.7$.^[14] Finally, Figure 2d shows the combined effects.

It is seen that in the bare system (Figure 2a), the four transition states, ⁴**TS1** and ²**TS1** as well as ⁴**TS3** and ²**TS3**, are very close in energy ($E + \text{ZPE}$), whereas the environmental effects (Figure 2b–d) tip the balance in favor of hydroxylation. Thus, with just two hydrogen bonds (Figure 2b) away from the reaction center, the lowest transition state becomes ²**TS3**, the LS species for hydroxylation. When a polarization effect is applied (Figure 2c) the HS hydroxylation species ⁴**TS3** descends also below the epoxidation species. Finally, when both effects are combined (Figure 2d), the preference for hydroxylation further increases. In fact, the general trend is true without ZPE, as well as when free energies at different temperatures are considered (see Supporting Information). The calculated energy changes correspond to a regioselectivity change of at least two orders of magnitude. Furthermore, the environmental effects prefer the effectively concerted LS process for both reactions. Thus, the present study demonstrates that the stereospecificity and regioselectivity changes are emergent properties that can, in principle, originate in the electronic interaction exerted on the active species of the enzyme by the protein pocket.

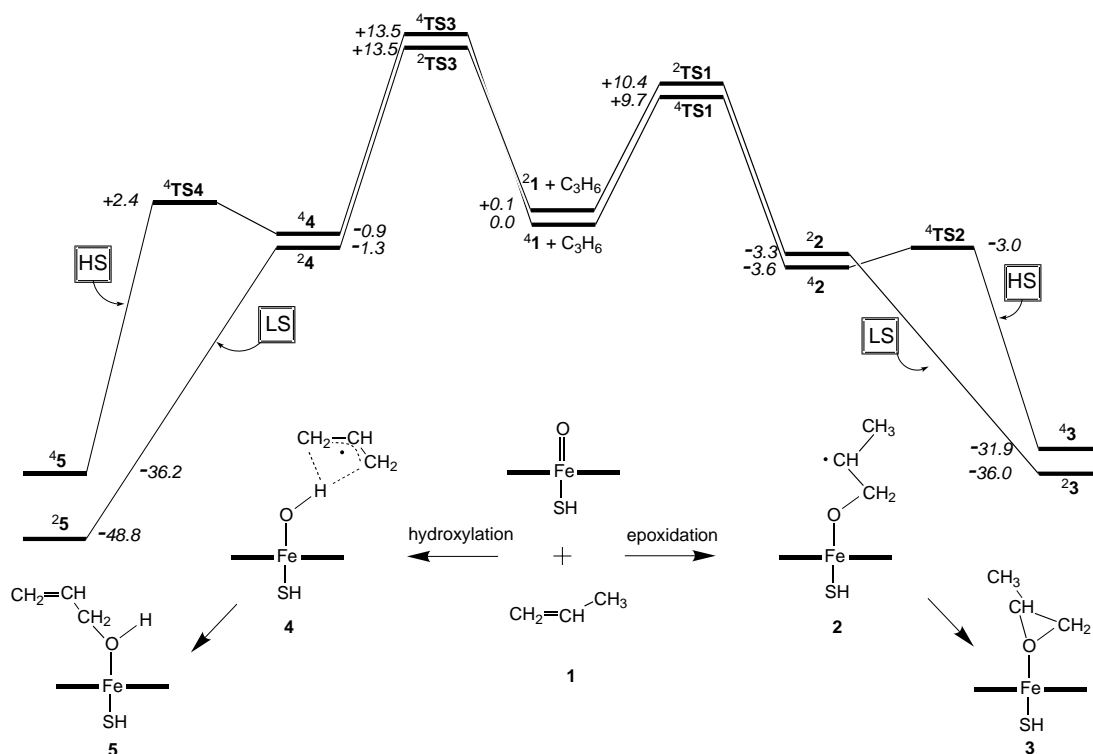


Figure 1. Energy profiles for hydroxylation and epoxidation of propene (energies in kcal mol^{–1}).

A straightforward comparison with experiment is not possible, since our calculations focus on the electronic component alone. Nevertheless, some general trends can be addressed. The calculated facility of C–H hydroxylation concurs with the opinion that the thiolate ligand enables P450 enzymes to carry out hydroxylations of nonactivated C–H bonds.^[3, 15] The calculations show, however, that this function is made more selective by the NH⋯S bonding machinery and the electric field of the protein. The calculated C=C/C–H ratio is 0.007–0.11, and falls within the range of observed values.^[6, 8] Moreover, in line with the preference for the LS processes, experimental data show that alkane hydroxylation by P450 isozymes occurs with high degrees of stereoselectivity, albeit incomplete.^[1, 3] Similarly, epoxidations of *cis*- and *trans*-butenes by a few P450 isozymes were shown^[16] to be stereospecific. An experimental study that addresses the effect of NH⋯S hydrogen bonding on the ratio of C–H hydroxylation to C=C epoxidation, shows that in P450_{cam},^[6] two hydrogen bonds are slightly more favorable for hydroxylation than three. While this is not directly comparable to the results of our calculations, it nevertheless shows that the NH⋯S hydrogen bonds apply a subtle effect on the reaction center.

Insight into the origins of the computed environmental effects can be gained from Figure 3 and 4. Figure 3 shows the bond activation transition state structures, along with two indicators of their electronic features, the transition state dipole moments (μ) and their polarizabilities (α). For each process, larger dipole moments and polarizabilities are possessed by the LS transition states. Moreover, the hydroxylation transition states are significantly more polarizable than those of the epoxidation species. It seems that the polarizability is the more important factor, and comes into play especially through the localized NH⋯S hydrogen-bonding interactions. Consequently, the most highly affected species is the most polarizable one, the LS hydroxylation species, ²TS3, which becomes the lowest transition state.^[17]

To understand the roots of this behavior of the system, consider first Cpd I. As shown recently,^[14] the electronic structure of Cpd I can be reconstructed as a hybrid of the resonance structures **a** and **b** (Figure 4A). In both structures there are three unpaired electrons: two in the π^* (d_{xz} , d_{yz}) orbitals of the FeO moiety and the third one is located either in a porphyrin (Por) orbital (a_{2u}) in structure **a**, or in a sulfur hybrid orbital in

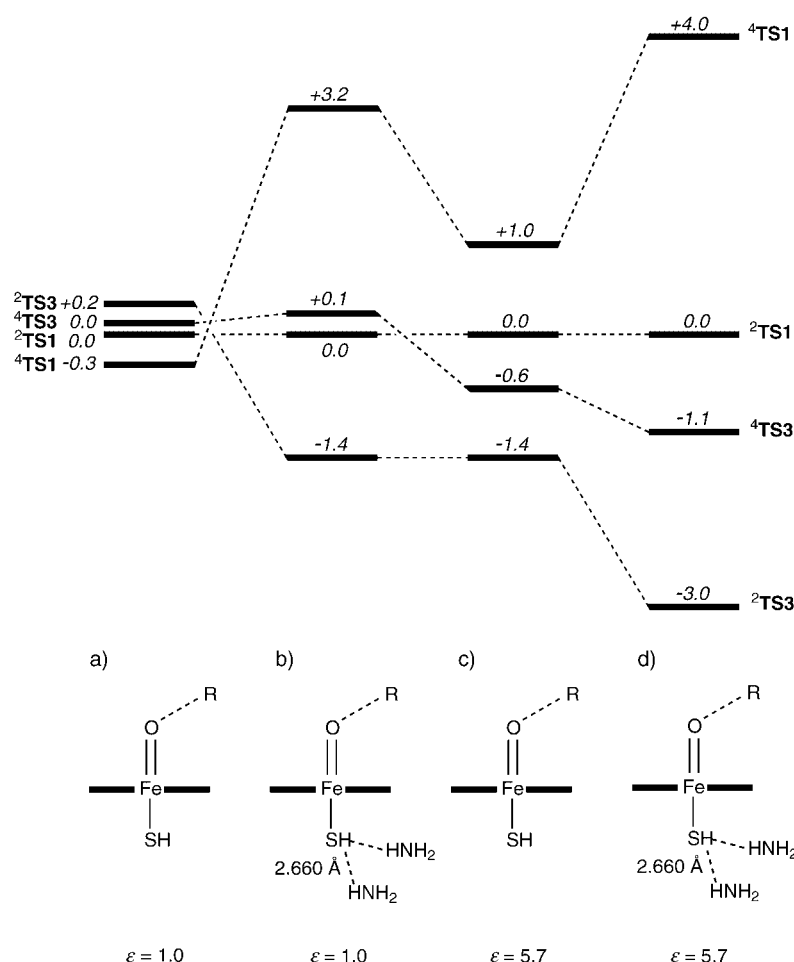


Figure 2. Relative energies (including ZPE) of the bond-activation transition states, ⁴TS1 and ²TS1 as well as ⁴TS3 and ²TS3 (R is the propene moiety); a) $\epsilon=1$ refers to the gas-phase situation, b) bare molecules with NH⋯S hydrogen bonds, c) molecules in a polarizing medium of $\epsilon=5.7$, and d) combined effects of b) and c). Energies are in kcal mol⁻¹, relative to ²TS1.

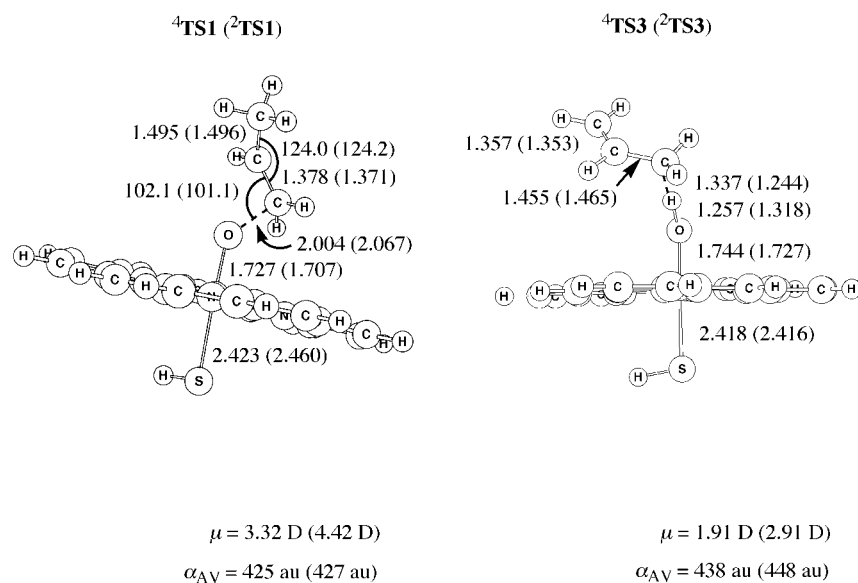


Figure 3. Geometries of the bond-activation transition states. Bond lengths are in Å. The pairs of data refer to the high-spin species and the low-spin species (in parentheses). Below the structures we specify dipole moment (μ) in Debye units, and the average electronic polarizability (α_{AV}) in atomic units.

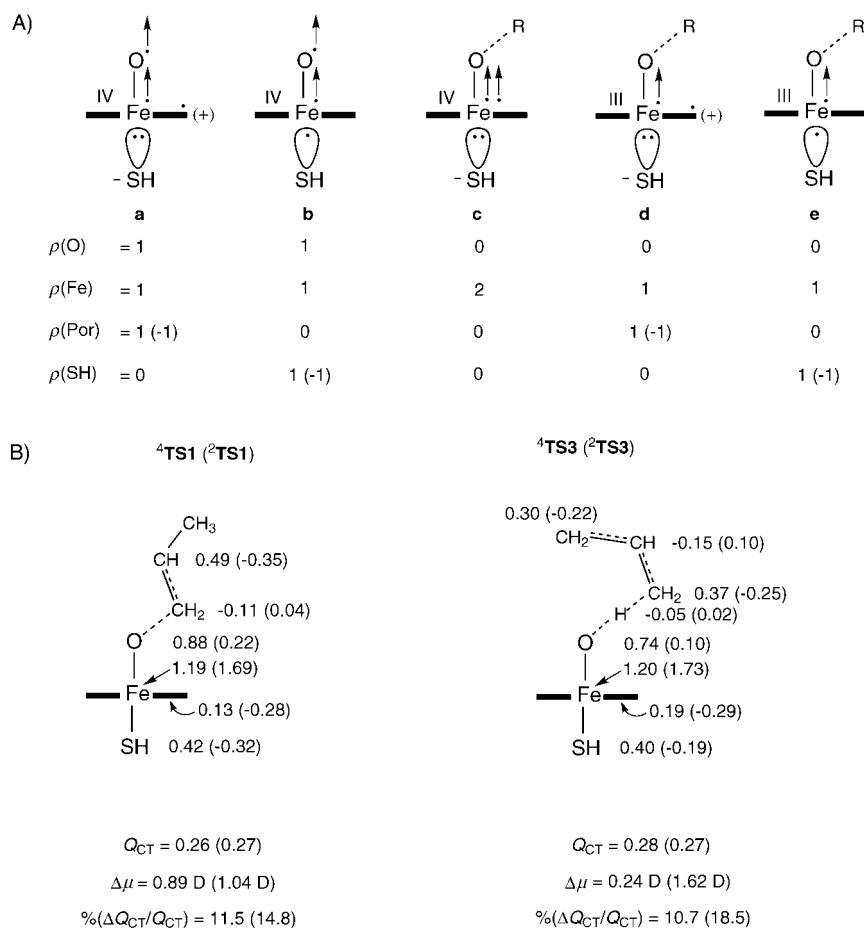


Figure 4. A) Some of the resonance forms that contribute to the chameleonic nature of the transition states (**TS**), and their idealized group spin densities, ρ (ρ values in parentheses correspond to the LS situation). B) Spin densities in ²TS1 and ⁴TS1 as well as ²TS3 and ⁴TS3, degrees of charge transfer (Q_{CT}) in units of electrons, changes in dipole moments ($\Delta\mu$) and in degree of charge transfer ($\% \Delta Q_{\text{CT}}/Q_{\text{CT}}$), induced by the two NH...S hydrogen bonds. The pairs of data refer to the high-spin species (out of parentheses) and low-spin ones (in parentheses).

structure **b**.^[14,18] Whereas the bare system is **b**-like, medium polarization and NH...S hydrogen bonding stabilize structure **a**. The stronger the hydrogen bonding and the polarizing effect, the more **a**-like is Cpd I. Thus, Cpd I, the reactant of the two oxidation processes, behaves as a chameleon state that changes character to fit the environment into which it is accommodated.

Transition states are generally more polarizable than their reactants and products, owing to electronic delocalization in the bonds that are broken and formed during the reaction. However, the transition states of the P450 oxidation are special, since in addition they also possess available orbitals on the iron center, the porphyrin, and the thiolate moieties. These orbitals are not fully occupied and are also close in energy, and can therefore participate in delocalizing the electrons in the transition state, thereby making the transition state very polarizable. A similar idea was articulated by experimentalists.^[2-5, 19]

In addition to **a** and **b**, among the many other resonance structures that contribute to electron delocalization in the transition state, three important reference forms are those that represent the flavors of the reaction intermediates (**2** and

4, Figure 2), and are depicted in **c–e** in Figure 4A.^[12] One form is the Fe^{IV} species (**c**) and the other two forms are the singlet and triplet Fe^{III} species shown in **d** and **e**. The computed transition states spin density, on iron, in Figure 4B is seen to reflect different blends of **c–e**. In the HS species, ⁴TS3 and ⁴TS1, the spin density on Fe (ca 1.2) is closer to the situation in Fe^{III}, while in ²TS1 and ²TS3, this spin density (ca 1.7) is closer to the situation in Fe^{IV}. In addition to these contributions, there are resonance forms in which the propene transfers an electron to the available low-lying orbitals of the Cpd I moiety. The quantity Q_{CT} in Figure 4B shows that the degree of charge transfer from the propene is about 0.26–0.28 e[−], which in turn means that the charge transfer forms constitute some 26–28% of the transition state character, and will generally vary with the donor capability of the substrate. Clearly, the transition states are richly blended in terms of closely lying resonance structures, and this rich blend endows them with high polarizability and response to the protein environment.

To summarize the changes imparted by the environment most succinctly, we indicate below the structures in Figure 4B, the computed changes in the dipole moment and in the percentages of charge transfer, when ⁴TS1 and ²TS1 as well as ⁴TS3 and ²TS3 are subject to NH...S hydrogen bonds. These changes are seen to be larger for the LS species ²TS1 and ²TS3 than for the HS counterparts. Especially large changes are apparent in the dipole moments of the LS

hydroxylation species, ²TS3 that changes its dipole by as much as 1.62 D upon hydrogen bonding to the thiolate. Apparently, the variable blend of resonance structures endows the transition states with a chameleonic nature. It follows therefore that not only is Cpd I a chameleon species, it is also a chameleon oxidant that tunes its reactivity and selectivity patterns in response to the protein environment in which it is accommodated.

Our study is a first principle demonstration that, in addition to classical factors (such as active species accessibility, substrate fit, and steric effects^[1, 8, 9]), there is a significant electronic component that modulates regioselectivity of oxidation by P450 enzymes. This factor is the chameleonic character of the active species that varies in response to the hydrogen-bonding machinery of the protein pocket and its polarity. Especially notable is the effect of the NH...S hydrogen bonding, which exerts its influence on the Fe=O reaction center from the remote proximal side. Thus, a single oxidant having chameleon character like Cpd I, can in principle exhibit a library of reactivity patterns, depending on the electric and hydrogen-bonding properties of the protein pocket.

Methods

The calculations were performed with JAGUAR 4.1,^[20a] following previously established procedures.^[11, 12, 14] The calculations utilized the hybrid B3LYP density functional and the double zeta basis set, LACVP(Fe)/6-31G(C,H,N,O). Geometries were optimized and characterized by frequency calculations. To consider the pure environmental effect, the calculations (with hydrogen bonding and with $\epsilon = 5.7$) did not involve geometry re-optimization. The ZPEs (calculated with the more accurate Gaussian98 routine^[20b]) of the bare systems were added to the total energies for the different conditions in Figure 2.

Received: March 20, 2002 [Z18940]

- [1] *Cytochrome P450: Structure, Mechanisms and Biochemistry*, 2nd ed. (Ed.: P. R. Ortiz de Montellano), Plenum, New York, **1995**.
- [2] J. T. Groves, Y.-Z. Hang in *Cytochrome P450: Structure, Mechanisms and Biochemistry*, 2nd ed. (Ed.: P. R. Ortiz de Montellano), Plenum, New York, **1995**, chap. 1, p. 3.
- [3] W.-D. Woggon, *Top. Curr. Chem.* **1996**, *184*, 39–95.
- [4] M. Sono, M. P. Roach, E. D. Coulter, J. H. Dawson, *Chem. Rev.* **1996**, *96*, 2841–2887.
- [5] B. Meunier, J. Bernadou, *Struct. Bonding* **2000**, *97*, 3–35.
- [6] S. Yoshioka, S. Takahashi, K. Ishimori, I. Morishima, *J. Inorg. Biochem.* **2000**, *81*, 141–151.
- [7] T. L. Poulos, J. C. Vickery, H. Li in *Cytochrome P450: Structure, Mechanisms and Biochemistry*, 2nd ed. (Ed.: P. R. Ortiz de Montellano), Plenum, New York, **1995**, chap. 4, p. 125.
- [8] a) R. E. White, J. T. Groves, G. A. McClusky, *Acta Biol. Med. Ger.* **1975**, *38*, 475–482; b) R. T. Ruettinger, A. J. Fulco, *J. Biol. Chem.* **1981**, *256*, 5728–5734.
- [9] E. J. Mueller, P. J. Lioda, S. G. Sligar in *Cytochrome P450: Structure, Mechanisms and Biochemistry*, 2nd ed. (Ed.: P. R. Ortiz de Montellano), Plenum, New York, **1995**, chap. 3, p. 83.
- [10] J. J. Devos, O. Sibbeseb, Z. Zhang, P. R. Ortiz de Montellano, *J. Am. Chem. Soc.* **1997**, *119*, 5489–5498.
- [11] F. Ogliaro, N. Harris, S. Cohen, M. Filatov, S. P. de Visser, S. Shaik, *J. Am. Chem. Soc.* **2000**, *122*, 8977.
- [12] S. P. de Visser, F. Ogliaro, N. Harris, S. Shaik, *J. Am. Chem. Soc.* **2001**, *123*, 3037.
- [13] S. Shaik, M. Filatov, D. Schröder, H. Schwarz, *Chem. Eur. J.* **1998**, *4*, 193–198.
- [14] F. Ogliaro, S. Cohen, S. P. de Visser, S. Shaik, *J. Am. Chem. Soc.* **2000**, *122*, 12 892.
- [15] T. Ohno, N. Suzuki, T. Dokoh, Y. Urano, K. Kikuchi, M. Hirobe, T. Higuchi, T. Nagano, *J. Inorg. Biochem.* **2000**, *82*, 123–125.
- [16] A. D. N. Vaz, D. F. McGinnity, M. J. Coon, *Proc. Natl. Acad. Sci. USA* **1998**, *95*, 3555–3560.
- [17] A pioneering study of the effect of the protein electric field on the resting state of P450 is given in: D. Harris, G. Loew, *J. Am. Chem. Soc.* **1993**, *115*, 8775–8779.
- [18] D. L. Harris, *Curr. Opin. Chem. Biol.* **2001**, *5*, 724–735.
- [19] R. Weiss, D. Mandon, T. Wolter, A. X. Trautwein, M. Muther, B. Eckhard, A. Gold, K. Jayaray, J. Turner, *J. Biol. Inorg. Chem.* **1996**, *1*, 377.
- [20] a) Jaguar 4.1. Portland OR, **1998**; b) Gaussian98 (Revision A.7), M. J. Frisch, G. W. Trucks, H. B. Schlegel, G. E. Scuseria, M. A. Robb, J. R. Cheeseman, V. G. Zakrzewski, J. A. Montgomery, R. E. Stratmann, J. C. Burant, S. Dapprich, J. M. Millam, A. D. Daniels, K. N. Kudin, M. C. Strain, O. Farkas, J. Tomasi, V. Barone, M. Cossi, R. Cammi, B. Mennucci, C. Pomelli, C. Adamo, S. Clifford, J. Ochterski, G. A. Petersson, P. Y. Ayala, Q. Cui, K. Morokuma, D. K. Malick, A. D. Rabuck, K. Raghavachari, J. B. Foresman, J. Cioslowski, J. V. Ortiz, B. B. Stefanov, G. Liu, A. Liashenko, P. Piskorz, I. Komaromi, R. Gomperts, R. L. Martin, D. J. Fox, T. Keith, M. A. Al-Laham, C. Y. Peng, A. Nanayakkara, C. Gonzalez, M. Challacombe, P. M. W. Gill, B. G. Johnson, W. Chen, M. W. Wong, J. L. Andres, M. Head-Gordon, E. S. Replogle, J. A. Pople, Gaussian, Inc., Pittsburgh, PA, **1998**.

A Dynamic Rearrangement of a Metal Cluster in a Process that Closely Resembles the Hopping Mechanism of Adatom Diffusion on Metal Surfaces**

Richard D. Adams,* Burjor Captain, Wei Fu, Perry J. Pellechia, and Mark D. Smith

It has been over 20 years since Muetterties proposed the widely discussed cluster–surface analogy as a model for understanding surface phenomena on an atomic level.^[1–5] Over the years, however, there have been surprisingly few well-characterized experimental confirmations of this concept.^[6–8] One important surface process that has been well studied over the years is that known as adatom diffusion.^[9–12] Adatom diffusion is important to understanding crystal and thin-film growth, phase transitions, segregation, cluster nucleation, and other surface phenomena. The two most important mechanisms are atom hopping and atom exchange.^[9–11]

In the atom hopping mechanism, an adatom moves from one hollow site to another by moving over a pair of atoms via an “edge bridge” twofold transition state, see the fourfold, twofold, fourfold example in Figure 1.

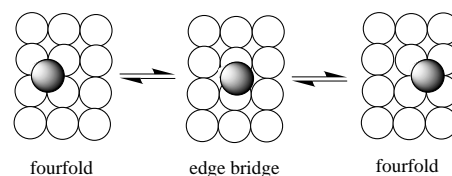


Figure 1. The shaded surface adatom moves from one fourfold site to another via an edge-bridging transition state.

Here we report the synthesis and molecular structures of the compound $[\text{PtRu}_5(\text{CO})_{15}(\text{PtBu}_3)(\text{C})]$ (**1**) and a study of its unusual molecular dynamics in solution by variable temperature NMR spectroscopy.^[13] Compound **1** was obtained in 52 % yield from the reaction of $[\text{Ru}_5(\text{CO})_{15}(\text{C})]$ ^[14] with $[\text{Pt}(\text{PtBu}_3)_2]$ ^[15] at 25 °C.^[16] The compound crystallizes in three different crystal modifications depending on the solvent that is used. Mixtures of a triclinic form and a monoclinic form **A** were observed to form by crystallization from solutions in benzene/octane solvent mixtures.^[17, 18] The molecular structure of the compound is similar in both of these crystal forms and the structure consists of a square-pyramidal cluster of five ruthenium atoms with one platinum atom spanning the square base with significant bonding to the four proximate ruthenium atoms (Figure 2). The four Pt–Ru distances range from

[*] Dr. R. D. Adams, B. Captain, W. Fu, Dr. P. J. Pellechia, Dr. M. D. Smith
Department of Chemistry and Biochemistry and USC Nanocenter
University of South Carolina
Columbia, SC 29208 (USA)
Fax: (+1) 803-777-6781
E-mail: Adams@mail.chem.sc.edu

[**] This work was supported by the Office of Basic Energy Sciences, US Department of Energy.